http://dx.doi.org/10.5012/bkcs.2013.34.12.3570

Synthesis of Poly(methacrylic acid)-functionalized SBA-15 and its Adsorption of Phenol in Aqueous Media

Vien Vo,[†,‡] Hee-Jin Kim,[†] Ha-Yeong Kim,[†] Youngmee Kim,[†] and Sung Jin Kim[†,*]

[†]*Department of Chemistry and Nano Science, Ewha Womans University, Seoul 120-750, Korea.* [*]*E-mail: sjkim@ewha.ac.kr*
[‡]*Department of Chemistry, Quy Nhon University, Viet Nam*
Received August 5, 2013, Accepted September 2, 2013

Poly(methacrylic acid)-functionalized SBA-15 silicas (denoted as P-x-PMA/SBA-15 where x is molar ratio of TSPM/(TEOS+TSPM) in percentage in the initial mixture) were synthesized by co-condensation of tetraethoxysilane and varying contents of 3-(trimethoxysilyl)propyl methacrylate in acidic medium with the block copolymer Pluronic 123 as a structure directing agent and then polymerization by methacrylic acid in the presence of ammonium persulfate as an initiator. The functionalized materials were characterized by PXRD, TEM, SEM, IR, and N_2 adsorption-desorption at 77 K. The investigation of phenol adsorption in aqueous solution on the materials showed that the poly(methacrylic acid)-functionalized mesoporous silicas possess strong adsorption ability for phenol with interaction of various kinds of hydrogen bonds. The adsorption data were fitted to Langmuir isotherms and the maximum adsorption capacity of the three functionalized materials P-5-PMA/SBA-15, P-10-PMA/SBA-15, and P-15-PMA/SBA-15 to be 129.37 mg/g, 187.97 mg/g, and 78.43 mg/g, respectively, were obtained. The effect of the pH on phenol adsorption was studied.

Key Words : Mesoporous materials, Functionalization, Methacrylate, Phenol adsorption

Introduction

Since the discovery of M41S silica in 1992, mesoporous materials have received considerable attention because of their large surface areas, well-defined pore structures, inert framework, nontoxicity and high biocompatibility.[1,2] However, most of the silicate-based mesoporous inorganic solids are synthesized by using the tetraethoxysilane $Si(OC_2H_5)_4$ (TEOS) as a silicate source, and they exhibit relatively low chemical activity. Therefore, by introducing the silane coupling agents with different functional groups as silicate sources, new mesoporous materials with novel properties may be obtained, which can be useful in a wide range of applications, such as in catalysis, adsorption, separation, chemical sensing, luminescence and drug delivery systems.[3-7]

Among the mesoporous materials, SBA-15 has gained considerable attention as an ideal host for incorporation of active molecules due to their large pore-size mesochannels with thick walls, adjustable pore size from 3 to 30 nm and high hydrothermal and thermal stability.[8-12] In order to remove toxic heavy-metal ions from aqueous solutions, the functionalization of mesostructured materials has been intensively investigated.[13,14] For this purpose, some organic functional groups such as thiol, amine, have been used to graft or incorporate onto the surface of SBA-15 mesopore channels using ligand-functionalized organosilanes.[15-17] However, only few studies on functionalized mesoporous silicas for adsorption of organic pollutants have been reported.[18,19]

The surface and ground water polluted by various chemicals may be caused by the rapid growth of the chemical and petrochemical industries. Among the organic chemicals, phenols are classified as highly toxic, harmful to living organisms even at low concentrations. The presence of phenols in the environment may come from the various ways of industrial processes, such as oil refining, petrochemical production, ceramic manufacturing, coal conversion and the phenolic resin industry.[20] To remove organic pollutants from aqueous solutions, many methods such as adsorption, chemical oxidation, precipitation, distillation, solvent extraction, ion exchange, membrane processes, and reverse osmosis have been investigated.[21] However, among them, adsorption has been used widely because of its significant advantages, including high efficiency, ease of handling, high selectivity, low operating costs, easy regeneration of adsorbent, and minimal generation of chemical or biological sludge.[21,22] For removal of phenol in water, some materials, such as resin,[23] activated carbon,[24] red mud,[25] rubber seed coat,[26] clay minerals,[27] and other materials have been studied. The reports showed that the adsorption process is strongly affected by surface chemistry and morphology of the adsorbents. Therefore, new adsorbents, which are economical, having strong affinity and high uptake capacity, have been raised.

Poly(methacrylic acid) has been used for wastewater treatment,[28,29] removal of metal ion,[30-33] selective adsorption of hemoglobin[34] and adsorption of organic compounds in water reported in the papers.[35,36] Strong hydrogen-bond interaction can be formed between methacrylic acid and phenol through a great number of carboxyl groups on its macromolecular chains.[35] In this work, SBA-15 silicas were functionalized by varying proportions of 3-(trimethoxysilyl)propyl methacrylate through one-pot synthesis, and then polymerized by methacrylic acid in the presence of ammonium persulfate ($(NH_4)_2S_2O_8$) as an initiator. The phenol

adsorption on the functionalized materials has been also investigated.

Experimental

Chemicals. Triblock copolymer Pluronic P123 ($HO(CH_2CH_2O)_{20}(CH_2CH(CH_3)O)_{70}(CH_2CH_2O)_{20}H$), tetraethyl orthosilicate ($(C_2H_5O)_4Si$, TEOS) and 3-(trimethoxysilyl)-propyl methacrylate ($CH_2=C(CH_3)COO(CH_2)_3Si(OCH_3)_3$, TSPM), methacrylic acid, ammonium persulfate were purchased from Merck. Hydrochloric acid was purchased from Shanghai Chemical Company. All chemicals were used as received without any further purification.

Synthesis. Poly(methacrylic acid)-functionalized SBA-15 samples were synthesized by a two-step procedure. Firstly, 3-(trimethoxysilyl)propyl methacrylate-functionalized SBA-15 samples were synthesized by a procedure reported in our previous paper.[37] In a typical process, 2 g of P123 were added to 62.5 g of HCl 1.9 M with stirring. 3.84 g of TEOS was added after the mixture was heated to 40 °C. An appropriate amount of TSPM was added after the mixture was stirring for 2 h. Three different molar ratios of TSPM/(TEOS+TSPM) of 0.05, 0.10 and 0.15 were used in three initial mixtures, individually. The reaction mixture was stirred for 20 h at 40 °C, and then aged in an autoclave at 100 °C for 24 h. The solid products were separated by filtration, and washed with water several times. The structure directing agent (P123) was removed by using ethanol extraction at 70 °C for 24 h. These obtained materials are denoted as x-PMA/SBA-15, where x is referred as the molar ratio of TSPM/(TEOS+TSPM) in percentage in the initial mixture. In the second step, 1 g of x-PMA/SBA-15 and 4 g of methacrylic acid were added into 70 mL of water. The mixture was stirred and heated to 70 °C under N_2 atmosphere, and then 0.002 g of ammonium persulfate was added to the mixture. The resulting mixture was stirred further for 24 h at 70 °C under N_2 atmosphere. The solid (P-x-PMA/SBA-15) was isolated by filtration and extracted with ethanol to remove the polymers attached physically to the surface. The general synthesis process of P-x-PMA/SBA-15 is expressed in Figure 1. For comparison, pure SBA-15 silica was also synthesized following the procedure of the first step without addition of TSPM.

Characterization. X-ray diffraction (XRD) for the samples were measured on the Brucker D8 Advance diffractometer using CuKα radiation (λ = 1.5406 Å). Transmission electron microscopy (TEM) and scanning electron microscopy (SEM) images were recorded on JEOL JEM-2100F and JEOL 5410, respectively. N_2 adsorption–desorption isotherms were obtained on ASAP 2010 at 77 K. Before the measurement, the samples were degassed at 100 °C for 6 h. Infrared (IR) spectra for the samples were recorded on a Thermo Nicolet spectrometer.

Phenol Adsorption. The effect of contact time, initial phenol concentration, and pH of the aqueous solution on the adsorption of phenol was investigated with the various sets. Single runs were carried out by stirring 50 mg of the adsorbent in 20 mL of aqueous phenol solution at 30 °C. The adsorbents after the adsorption procedure were separated through centrifugation. The concentration of the remaining phenols in the supernatant was determined by UV absorption spectroscopy (absorption λ_{max} at 269 nm) with a SCINCO S-4100 PDA UV-Vis spectrophotometer. The phenol adsorption capacity was determined by the difference between the initial and final phenol concentrations in the solution. The influence of pH on the adsorption property of P-x-PMA/SBA-15 was examined with solutions having various pH values. The pH was measured with a pH meter (pH-200L, NEOMET).

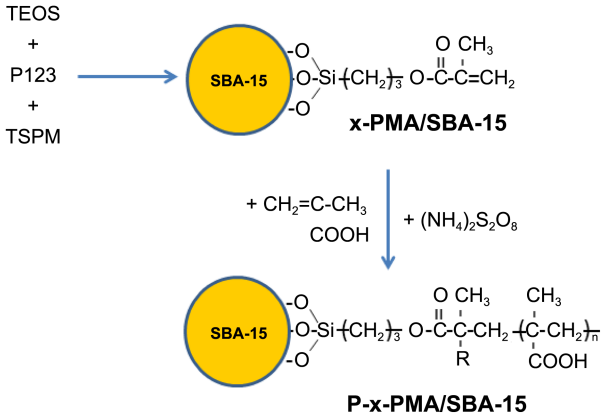

Figure 1. Synthesis diagram of P-x-PMA/SBA-15 materials.

Results and Discussion

Characterization of Adsorbents. The small-angle X-ray diffraction patterns of pure SBA-15, and the functionalized materials P-5-PMA/SBA-15, P-10-PMA/SBA-15, and P-15-PMA/SBA-15 are displayed in Figure 2. For the pure SBA-15, three resolved diffraction peaks with 2θ at 0.92°, 1.61° and 1.87°, indexed as (100), (110) and (200) reflections, were clearly observed, indicative of a two dimensional hexa-

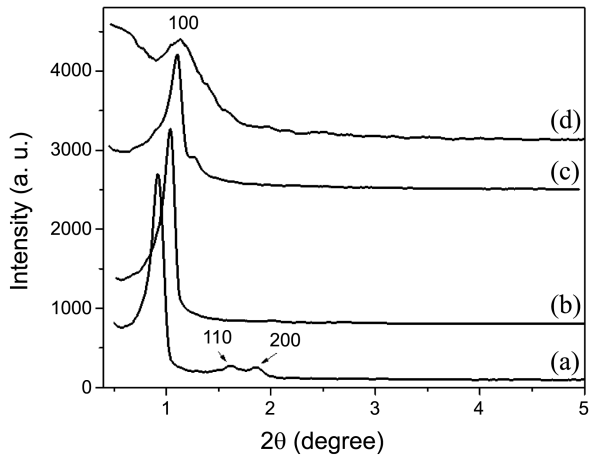

Figure 2. Powder low-angle XRD patterns of the pure SBA-15 (a), P-5-PMA/SBA-15 (b), P-10-PMA/SBA-15 (c), and P-15-PMA/SBA-15 (d).

gonal lattice with high p*6mm* symmetry.[12] The functionalized materials exhibit an intensive reflection (100), indicating the presence of ordered hexagonal structure similar to the pure SBA-15 silica. However, the peak intensity decreased significantly and the (110) and (200) reflections disappeared. The peak intensity decreased with increasing TSPM content in the gels. This is probably due to the decreased long-range structural ordering resulting from disturbed self-assembly of surfactant and silica precursor by TSPM during synthesis process and the decreasing scatter contrast between the silica framework and the organic moieties.[38,39] In addition, at high contents, the inclusion of methacrylate groups also contributes to increased disorder.

Figure 2 also shows the influence of TSPM concentration in the gel on the *d*-values in the X-ray diffraction patterns. A steady decrease in the d_{100} value was observed upon cocondensation with increasing TSPM content. From the (100) reflections, the hexagonal lattice parameters, $a = 2d_{100}/3^{1/2}$, were calculated to be reduced gradually by increasing TSPM as reported in Table 1.

The periodicity in the mesostructure of the P-x-PMA/SBA-15 materials was confirmed directly by transmission electron microscopy (Fig. 3). The TEM micrographs show both the perpendicular and parallel channels relative to the longitudinal axis observed, which confirms that the functionalized SBA-15 materials contain ordered, one-dimensional pore structure, similar to that of the pure SBA-15. However, a gradual decrease in structural ordering with TSPM content can be seen from the images of channels in Figue 3. The morphology of rope-like domains with a uniform size has been obtained for all the materials (Fig. 4). However, the surface becomes rougher and particle size decreases with increasing content of TSPM.

The N_2 adsorption/desorption isotherms at 77 K as well as the pore size distributions of the calcined SBA-15 and the functionalized SBA-15 samples are shown in Figure 5. The type IV IUPAC isotherms, characteristic of capillary condensation in mesopores have been found for all samples except for P-15-PMA/SBA-15. Their shapes are different

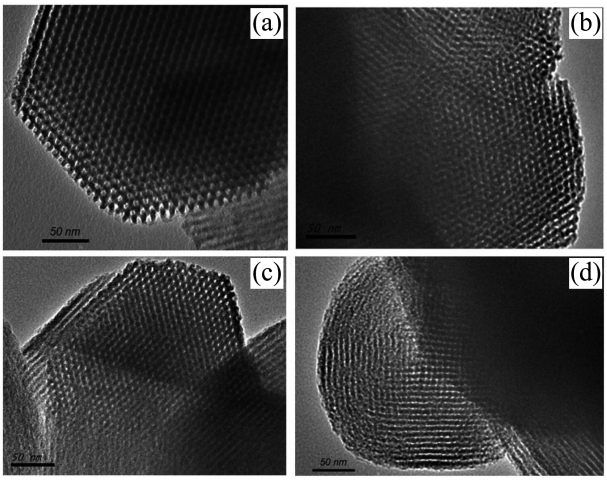

Figure 3. TEM images of the pure SBA-15 (a), P-5-PMA/SBA-15 (b), P-10-PMA/SBA-15 (c), and P-15-PMA/SBA-15 (d).

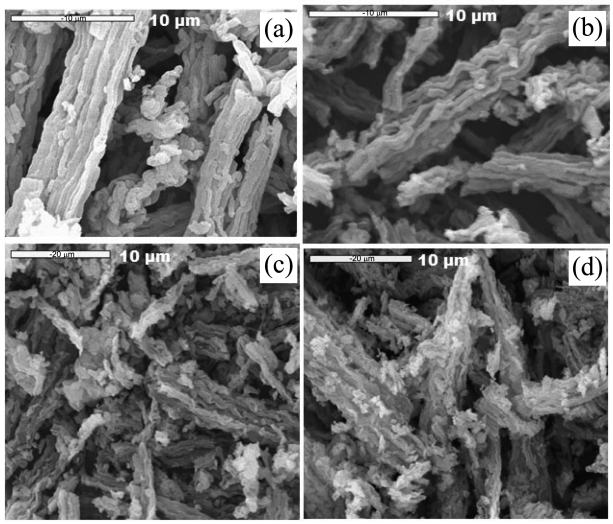

Figure 4. SEM images of the pure SBA-15 (a), P-5-PMA/SBA-15 (b), P-10-PMA/SBA-15 (c), and P-15-PMA/SBA-15 (d).

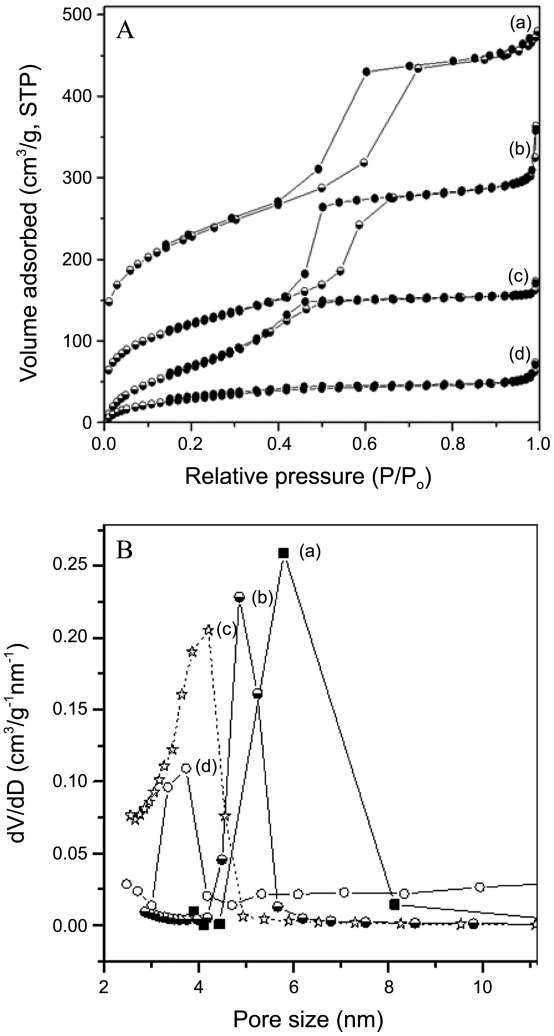

Figure 5. A: N_2 adsortion–desorption isotherms of the pure SBA-15 (a), P-5-PMA/SBA-15 (b), P-10-PMA/SBA-15 (c), and P-15-PMA/SBA-15 (d); B: Pore size distribution curves of the pure SBA-15 (a), P-5-PMA/SBA-15 (b), P-10-PMA/SBA-15 (c), and P-15-PMA/SBA-15 (d).

with a capillary condensation of N_2 occurring over a slightly lower P/P_0 range and a smaller pore volume with higher content of TSPM. The capillary condensation could not be observed for the sample P-15-PMA/SBA-15 with the highest TSPM content. Generally, a change in the shape of isotherms and the pore size distribution are observed when varying content of the functionalization agent in the gel. The specific surface area and pore size, calculated according to the BET and BJH methods, are presented in Table 1. A decrease in pore diameter, pore volume, and BET surface area (S_{BET}) with increasing TSPM content was obtained. Conversely, silica wall thickness extracted from the XRD and nitrogen sorption parameters steadily increases in the same order (Table 1). These results can be explained by the occupancy of poly(methacrylic acid) groups into the mesostructure. The above obtained data indicate the presence of organic groups and the preservation of SBA-15 textural properties, showing suitable porosity and surface for potential adsorbents.

To clarify the organic groups attached into the mesostructure, the materials were characterized by IR spectroscopy. As mentioned in Figure 1, to obtain the P-x-PMA/SBA-15 materials, we used a two-step procedure. In the first step, x-PMA/SBA-15 samples with methacrylate groups grafted on the surface were prepared. A polymerization process in the second step then was carried out between the methacrylate groups on the surface of x-PMA/SBA-15 and methacrylic acid in aqueous solution with the presence of ammonium persulfate as an initial agent to form P-x-PMA/SBA-15. To evidence the methacrylate groups grafted on the materials in the first step, the x-PMA/SBA-15 samples were characterized by IR spectroscopy and the results were shown in Figure 6(A). For comparison, also shown in the figure is the spectrum of P123. For P123, the peaks in the range of 2850-3000 cm^{-1} and at 1460 cm^{-1} corresponding to the C-H stretching and bending, respectively, and those at 1377 cm^{-1} and 1350 cm^{-1} coming from the stretching modes of C-O-C on P123 have been obtained.[40] For x-PMA/SBA-15 materials, these peaks became negligible, indicating that the surfactant in these materials was almost completely removed upon extraction with ethanol. The bands at 1630 cm^{-1} and 3450 cm^{-1} were attributed to vibration of the O-H bond of chemisorbed H_2O.[41] In addition to the peaks corresponding to the vibrational modes mentioned above, it is worth to know that a band at 1704 cm^{-1} appearing in all spectra of the three samples 5-PMA/SBA-15, 10-PMA/SBA-15 and 15-PMA/SBA-15 may be due to vibrational mode of C=O group.[42,43] The intensity of this peak increases with increasing content of TSPM in the reaction mixture. This demonstrates strongly that the carbonyl groups are grafted on the materials and the carbonyl contents are proportional to the TSPM contents in the initial mixture.

FTIR spectra of three functionalized SBA-15 samples are illustrated in Figure 6(B). As for the x-PMA/SBA-15 samples, the peaks corresponding to P123 were negligible and the new peak at 1704 cm^{-1} appeared in all spectra of the three samples P-5-PMA/SBA-15, P-10-PMA/SBA-15 and P-15-PMA/SBA-15. The intensity of this peak increases with

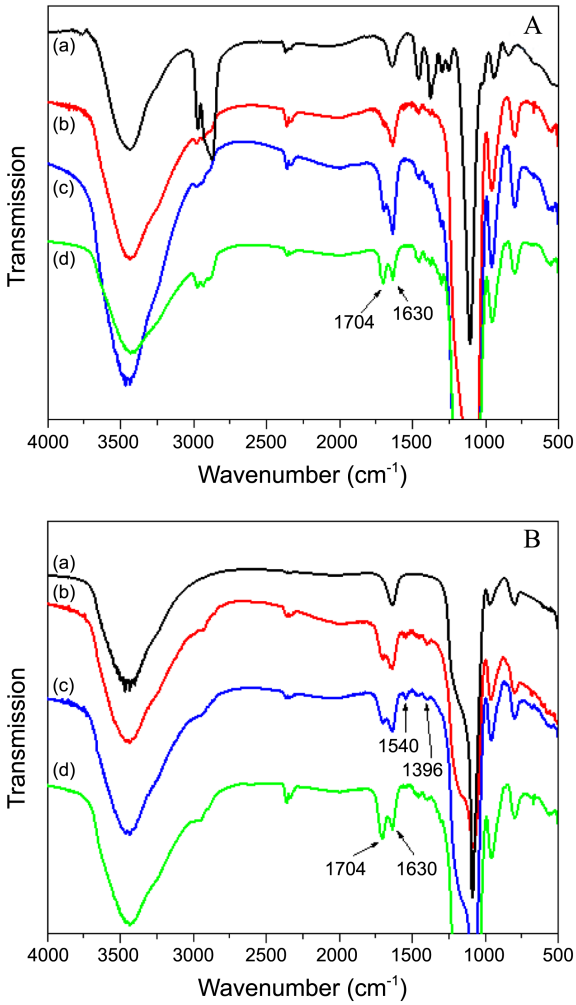

Figure 6. A: IR spectra of P123 (a), 5-PMA/SBA-15 (b), 10-PMA/SBA-15 (c), and 15-PMA/SBA-15 (d); B: IR spectra of the pure SBA-15 (a), P-5-PMA/SBA-15 (b), P-10-PMA/SBA-15 (c), P-15-PMA/SBA-15 (d).

increasing content of TSPM in the initial mixture. This result evidences strongly that the carbonyl groups are present in the functionalized materials and the carbonyl contents in the samples are proportional to the TSPM contents in the initial mixtures. It has been well known that the carbonyl stretch C=O of carboxylic acid appears as an intense band around 1700 cm^{-1}.[44-47] Therefore, the bands for C=O corresponding to TSPM and carboxylic acid of methacrylic acid may be overlapped each other in the peak at around 1704 cm^{-1}.

The occurrence of polymerization in the P-x-PMA/SBA-15 samples can be proved by comparison of intensity of the peaks at 1704 cm^{-1} for the x-PMA/SBA-15 samples in Figure 6(A) and those for the P-x-PMA/SBA-15 samples in Figure 6(B). Indeed, it can be seen from Figure 6 that ratio in intensity of the peak at 1704 cm^{-1} and 1602 cm^{-1} for the P-x-PMA/SBA-15 samples (Fig. 6(B)) is higher than that for the corresponding samples of x-PMA/SBA-15 (Fig. 6(A)). This may be supposed that the carbonyl group of carboxylic acid contributes to a relative increase in intensity of the peak at 1704 cm^{-1} for the P-x-PMA/SBA-15 samples. Besides, the

Table 1. Structural, textural properties of the pure SBA-15 and poly(methacrylic acid)-funtionalized SBA-15 materials

Material	S_{BET} (m^2/g)	Pore diameter (nm)	a (nm)	Wall thickness (nm)
SBA-15	438.5	6.4	11.1	4.7
P-5-PMA/SBA-15	404.6	4.8	9.8	5.0
P-10-PMA/SBA-15	358.0	4.2	9.3	5.1
P-15-PMA/SBA-15	177.1	3.7	9.0	5.3

appearance of peaks at 1540 cm^{-1} and 1396 cm^{-1} which are assigned to the asymmetric and symmetric -COO- stretching vibrations of carboxyl groups[46] may support further the presence of carboxylic acid group in the P-x-PMA/SBA-15 samples.

Phenol Adsorption.

Adsorption Equilibrium Time: The investigation on phenol adsorption for three functionalized-materials, P-5-PMA/SBA-15, P-10-PMA/SBA-15, and P-15-PMA/SBA-15 were carried out. In order to study the equilibrium time of adsorption, experiments were conducted on solutions containing initial different concentrations of phenol with pH of 7 in the presence of the adsorbent at 30 °C. The sample of each solution was collected and analyzed at the different times. Figure 7 shows that, with an initial phenol concentration of 100 mg/L, a strong adsorption was obtained within 8 h, after which the adsorption was nearly unchanged, and the equilibrium established at about 12 h for three P-5-PMA/SBA-15, P-10-PMA/SBA-15, P-15-PMA/SBA-15 samples. The same adsorption equilibrium times were also obtained for the initial phenol concentrations of 50 mg/L, 150 mg/L and 200 mg/L. However, we selected a stirring time of 24 h to obtain an absolute equilibrium for all subsequent adsorption experiments.

Adsorption Isotherms: To investigate isotherms for phenol adsorption on the P-5-PMA/SBA-15, P-10-PMA/SBA-15, and P-15-PMA/SBA-15 materials, equilibrium adsorption capacities of the materials at various initial concentrations of phenol at pH of 7 were studied. The data obtained were fitted to Langmuir Isotherms and the Langmuir linear plots are shown in Figure 8. From the linearized Langmuir equations, the values of maximum adsorption capacity for P-5-PMA/SBA-15, P-10-PMA/SBA-15, and P-15-PMA/SBA-15 were calculated to be 129.37 mg/g, 187.97 mg/g, and 78.43 mg/g, respectively. It can be seen from the data that the adsorption capacity decreases in the following order: P-10-PMA/SBA-15, P-5-PMA/SBA-15, and P-15-PMA/SBA-15. This can be explained by that a significant decrease in surface area of P-15-PMA/SBA-15 leads to the low adsorption capacity for this material. For P-5-PMA/SBA-15 and P-10-PMA/SBA-15 with insignificantly different values of surface area, the later has higher adsorption capacity may be due to the higher content of C=O and COOH groups than those of the earlier. To our knowledge, the adsorption capacity of 187.97 mg/g for P-10-PMA/SBA-15 is high compared to that (81.78 mg/g) for 10-PMA/SBA-15 in our previous work[37] and the other values (4.127–162.88 mg/g) reported.[21,25,26,34] This may indicate that the polymerization improves adsorption property of the P-x-PMA/SBA-15 material for phenol compared to that of the x-PMA/SBA-15 material. To confirm the key role of the functionalized groups in the P-x-PMA/SBA-15 materials for the phenol adsorption, SBA-15, refluxed by ethanol for removal of P123, was also investigated for phenol adsorption with the same process. The results showed that a negligible adsorption capacity for phenol on the SBA-15 (Fig. 7).

Influence of pH: For investigation on the influence of pH on the phenol adsorption, a representative sample, P-10-PMA/SBA-15, was studied with an initial concentration of phenol of 100mg/L and at temperature of 30 °C. The pH values of the initial solutions were varied from 2.5 to 10.5. Figure 9 shows that pH has a great influence on the adsorption property of the functionalized material for phenol. Generally, a decrease in adsorption of phenol for P-10-PMA/

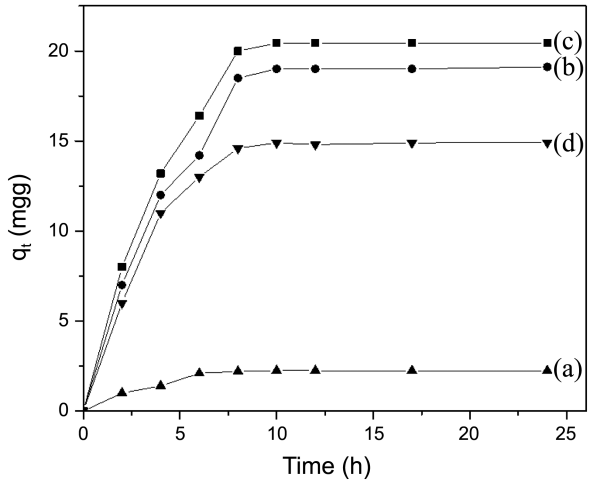

Figure 7. Effect of contact time for the adsorption of phenol onto the pure SBA-15 (a), P-5-PMA/SBA-15 (b), P-10-PMA/SBA-15 (c), and P-15-PMA/SBA-15 (d) with initial phenol concentration of 100 mg/L at 30 °C.

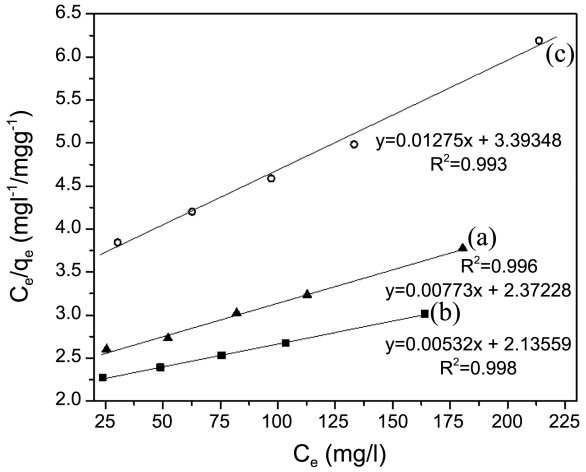

Figure 8. The Langmuir plots for the adsorption of phenol onto P-5-PMA/SBA-15 (a), P-10-PMA/SBA-15 (b), and P-15-PMA/SBA-15 (c) at 30 °C.

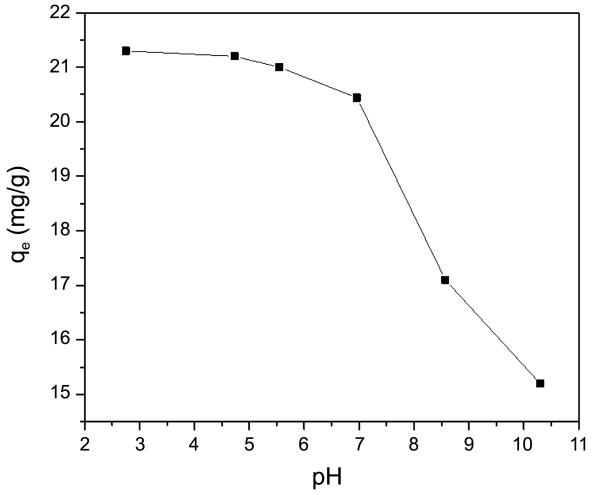

Figure 9. Effect of pH for the adsorption of phenol onto P-10-PMA/SBA-15 with initial phenol concentration of 100 mg/L at 30 °C.

SBA-15 with increasing the pH value from 2.5 to 10.5 was obtained. However, the decrease became strong at pH values over 7. This may be explained by the different kinds of hydrogen bond between C=O and COOH groups of the functionalized materials and phenol.[35] At low pH values, the carboxyl groups of P-10-PMA/SBA-15 and hydroxyl groups of phenol nearly do not dissociate, resulting in formation of the kinds of hydrogen bond. Therefore, the adsorption ability is strong and the adsorption capacity is high. On the contrary, increasing pH value leads to enhancement of dissociation degree of carboxyl groups of P-10-PMA/SBA-15 and hydroxyl groups of phenol, resulting in weakening and decrease of the kinds of hydrogen bond. This explains for decreasing adsorption capacity with increasing pH value. Especially, as pH > 7, carboxyl groups of P-10-PMA/SBA-15 and hydroxyl groups of phenol were neutralized, the kinds of hydrogen bond could not be formed. As a result, adsorption capacity dramatically decreases at pH values > 7. For the silanol groups of SBA-15, a very low adsorption capacity for phenol on SBA-15 as mentioned above may indicate a negligible interaction of these groups with phenol.

Conclusion

The poly(methacrylic acid)-functionalized SBA-15 materials with various contents of carbonyl and methacrylic acid groups were synthesized and investigated for adsorption of phenol from aqueous solutions. The equilibrium state for phenol adsorption in period of about 12 h was established. The adsorption data were fitted to Langmuir isotherms and the maximum adsorption capacity of 129.37 mg/g, 187.97 mg/g, and 78.43 mg/g were obtained for P-5-PMA/SBA-15, P-10-PMA/SBA-15, and P-15-PMA/SBA-15, respectively. The phenol adsorption of the functionalized material is affected by pH, and the uptake of phenol decreases with increasing pH value. The different kinds of hydrogen bond between C=O and COOH groups of the P-x-PMA/SBA-15 materials and hydrogen atom of phenol play a key role in the uptake of phenol on the fuctionalized materials.

Acknowledgments. This work was supported by the National Research Foundation of Korea (NRF) grant funded by the Korea government (MEST) (NRF-2011-0014219).

References

1. Beck, J. S.; Vartuli, J. C.; Roth, W. J.; Leonowicz, M. E.; Kresge, C. T.; Schmitt, K. D.; Chu, C. T. W.; Olson, D. H.; Sheppard, E. W.; McCullen, S. B.; Higgins, J. B.; Schlenker, J. L. *J. Am. Chem. Soc.* **1992**, *114*, 10834.
2. Kresge, C. T.; Leonowicz, M.; Roth, W. J.; Vartuli, J. C.; Beck, J. C. *Nature* **1992**, *359*, 710.
3. Kresge, C. T.; Leonowicz, M.; Roth, W. J.; Vartuli, J. C.; Beck, J. C. *Nature* **1992**, *359*, 710.
4. Lasseter, T. L.; Clare, B. H.; Abbott, N. L.; Hamers, R. J. *J. Am. Chem. Soc.* **2004**, *126*, 10220.
5. Kim, E.; Kim, H. E.; Lee, S. J.; Lee, S. S.; Seo, M. L.; Jung, J. H. *Chem. Commun.* **2008**, *33*, 3921.
6. Dai, Z. H.; Bao, J. C.; Yang, X. D.; Ju, H. X. *Biosens. Bioelectron.* **2008**, *23*, 1070.
7. Giri, S.; Trewyn, B. G.; Stellmaker, M. P.; Lin, V. S. Y. *Angew. Chem. Int. Ed.* **2005**, *44*, 5038.
8. Yan, B.; Zhou, L.; Li, Y. *Colloids and Surfaces A: Physicochem. Eng. Aspects* **2009**, *350*, 147.
9. Yan, B.; Zhou, L.; Li, Y. *Colloids and Surfaces A: Physicochem. Eng. Aspects* **2009**, *350*, 147.
10. Agirrezabal-Telleria, I.; Requies, J.; Guemez, M. B.; Arias, P. L. *Appl. Catal. B: Environ.* **2012**, *169*, 115.
11. Zhu, J.; Xie, X.; Carabineiro, S. A. C.; Tavares, P. B.; Figueiredo, J. L.; Schomacker, R.; Thomas, A. *Energy Environ. Sci.* **2011**, *4*, 2020.
12. Zhao, D.; Huo, Q.; Feng, J.; Chmelka, B. F.; Stucky, G. D. *J. Am. Chem. Soc.* **1998**, *120*, 6024.
13. Dai, S.; Burleigh, M. C.; Ju, Y. H.; Gao, H. J.; Lin, J. S.; Pennycook, S. J.; Barnes, C. E.; Xue, Z. L. *J. Am. Chem. Soc.* **2000**, *122*, 992.
14. Brown, J.; Mercier, L.; Pinnavaia, T. J. *Chem. Commun.* **1999**, 69.
15. Jaroniec, C. P.; Sayari, A.; Kruk, M.; Jaroniec, M. *J. Phys. Chem. B* **1998**, *102*, 5503.
16. Antochshuk, V.; Jaroniec, M. *J. Phys. Chem. B* **1998**, *103*, 6252.
17. Anbia, M.; Amirmahmoodi, S. *Scientia Iranica C* **2011**, *18*, 446.
18. Baccile, N.; Babonneau, F. *Micropor. Mesopor. Mater.* **2008**, *110*, 534.
19. Inumaru, K.; Nakano, T.; Yamanaka, S. *Micropor. Mesopor. Mater.* **2006**, *95*, 279.
20. Huang, J.; Wang, X.; Jin, Q.; Liu, Y.; Wang, Y. *J. Environ. Manage.* **2007**, *84*, 229.
21. Buscaa, G.; Berardinelli, S.; Resini, C.; Arrighi, L. *J. Hazard. Mater.* **2008**, *160*, 265.
22. Ahalya, N.; Ramachandra, T. V.; Kanamadi, R. D. *Res. J. Chem. Environ.* **2003**, *7*, 71.
23. Ku, Y.; Lee, K C. *J. Hazard. Mater.* **2000**, *80*, 59.
24. Mukherjee, S.; Kumar, S.; Misra, A. K.; Fan, M. *Chem. Eng. J.* **2007**, *129*, 133.
25. Tor, A.; Cengeloglu, Y.; Aydin, M. E.; Ersoz, M. *J. Colloid Interface Sci.* **2006**, *300*, 498.
26. Rengaraj, S.; Moon, S.; Sivabalan, R.; Arabindoo, B.; Murugesan, V. *J. Hazard. Mater.* **2002**, *89*, 185.
27. Senturka, H. B.; Ozdesa, D.; Gundogdua, A.; Durana, C.; Soylakb, M. *J. Hazard. Mater.* **2009**, *172*, 353.
28. Tang, E.; Cheng, G. X.; Ma, X. L.; Pang, X. S.; Zhao, Q. *Appl. Surf. Sci.* **2006**, *252*, 5227.
29. Azhgozhinova, G. S.; Güven, O.; Pekel, N.; Dubolazov, A. V.; Mun, G. A.; Nurkeeva, Z. S. *J. Colloid Interface Sci.* **2004**, *278*,

155.
30. Anirudhan, T. S.; Rijith, S. *J. Environ. Radioactivity* **2012**, *106*, 8.
31. Huang, L.; Yuan, S.; Lv, Li; Tan, G.; Liang, B.; Pehkonen, S. O. *Journal of Colloid and Interface Science* **2013**, *405*, 171.
32. Anirudhan, T. S.; Rijith, S.; Tharun, A. R. *Colloids and Surfaces A: Physicochem. Eng. Aspects* **2010**, *368*, 13.
33. Wang, W. *Process Safety and Environmental Protection* **2011**, *89*, 127.
34. Anirudhan, T. S.; Rejeena, S. R. *Carbohydrate Polymers* **2013**, *93*, 518.
35. An, F.; Gao, B.; Feng, X. *Chem. Eng. J.* **2009**, *153*, 108.
36. An, F.; Feng, X.; Gao, B. *J. Hazard. Mater.* **2010**, *178*, 499.
37. Phuong, T. T. T.; Hang, T. D.; Hung, N. P.; Nga, N. T. V.; Kim, S. J.; Vo, V. *J Porous Mater.* **2012**, *19*, 295.
38. Wang, X.; Lin, K. S. K.; Chan, J. C. C.; Cheng, S. *J. Phys. Chem. B* **2005**, *109*, 1763.
39. Mercier, L.; Pinnavaia, T. J. *Chem. Mater.* **2000**, *12*, 188.
40. Chong, A. S. M.; Zhao, X. S. *J. Phys. Chem. B* **2003**, *107*, 12650.
41. Zhang, M.; Shi, L.; Yuan, S.; Zhao, Y.; Fang, J. *J. Colloid Interface Sci.* **2009**, *330*, 113.
42. He, J.; Xu, Y.; Ma, H.; Evans, D. G.; Wang, Z.; Duan, X. *Micropor. Mesopor. Mater.* **2006**, *94*, 29.
43. Moller, K.; Bein, T.; Fischer, R. X. *Chem. Mater.* **1999**, *11*, 665.
44. Milner, S. T. *Science* **1991**, *251*, 905.
45. Tang, Q. L.; Xu, Y.; Wu, D.; Sun, Y. H. *J. Solid State Chem.* **2006**, *179*, 1513.
46. Nakamoto, K. *Infrared and Raman Spectra of Inorganic and Coordinates Compounds*; Wiley: New York, 1978.
47. Victor, S. P.; Sharma, C. P. *Colloids and Surfaces B: Biointerfaces* **2013**, *108*, 219.